DOI: 10.1002/chem.200902563

A New Heteroleptic Ruthenium(II) Polypyridyl Complex with Long-Wavelength Absorption and High Singlet-Oxygen Quantum Yield

Qian-Xiong Zhou,[a, b] Wan-Hua Lei,[a] Jing-Rong Chen,[a] Chao Li,[a] Yuan-Jun Hou,[a] Xue-Song Wang,*[a] and Bao-Wen Zhang*[a]

Abstract: Ruthenium(II) polypyridyl complexes with long-wavelength absorption and high singlet-oxygen quantum yield exhibit attractive potential in photodynamic therapy. A new heteroleptic Ru^{II} polypyridyl complex, $[Ru(bpy)(dpb)(dppn)]^{2+}$ (bpy = 2,2′-bipyridine, dpb = 2,3-bis(2-pyridyl)benzoquinoxaline, dppn = 4,5,9,16-tetraazadibenzo[*a*,*c*]naphthacene), is reported, which exhibits a ^{1}MLCT (MLCT: metal-to-ligand charge transfer) maximum as long as 548 nm and a singlet-oxygen quantum yield as high as 0.43. Steady/transient absorption/emission spectra indicate that the lowest-energy MLCT state localizes on the dpb ligand, whereas the high singlet-oxygen quantum yield results from the relatively long ^{3}MLCT(Ru→dpb) lifetime, which in turn is the result of the equilibrium between nearly isoenergetic excited states of ^{3}MLCT(Ru→dpb) and $^3\pi\pi^*$(dppn). The dppn ligand also ensures a high binding affinity of the complex towards DNA. Thus, the combination of dpb and dppn gives the complex promising photodynamic activity, fully demonstrating the modularity and versatility of heteroleptic Ru^{II} complexes. In contrast, $[Ru(bpy)_2(dpb)]^{2+}$ shows a long-wavelength ^{1}MLCT maximum (551 nm) but a very low singlet-oxygen quantum yield (0.22), and $[Ru(bpy)_2(dppn)]^{2+}$ shows a high singlet-oxygen quantum yield (0.79) but a very short wavelength ^{1}MLCT maximum (442 nm).

Keywords: antitumor agents · bioinorganic chemistry · DNA cleavage · ligand design · ruthenium

Introduction

Photodynamic therapy (PDT) is a promising treatment modality for malignant tumors.[1] It involves the production of cytotoxic reactive oxygen species (ROS), mainly singlet oxygen ($^1O_2$), upon illumination of a photosensitizer with visible or near-infrared (NIR) light. An ideal photosensitizer should have a high quantum yield of $^1O_2$ and strong absorptivity within the phototherapeutic window of 600–900 nm, at which the tissue penetration of light is optimal.

Transition-metal complexes with DNA photocleavage activity have received significant attention for their potential use as DNA structural probes and as anticancer agents.[2] Among them, Ru^{II} polypyridyl complexes were extensively studied owing to their rich photophysical, photochemical, and redox properties.[3] So far, many Ru^{II} polypyridyl complexes have been confirmed to possess DNA photocleavage activities through an $^1O_2$ mechanism, thus exhibiting their PDT application potential.[4] However, most of them suffer from short-wavelength absorption, with the absorption maximum of the metal-to-ligand charge-transfer (MLCT) transition shorter than 500 nm, remarkably limiting their use in PDT. Ligands with delocalized π systems can provide Ru complexes with longer MLCT absorption.[5,6] However, the low energy gap often leads to a short excited-state lifetime, that is, the energy-gap law,[7] which is very unfavorable for $^1O_2$ generation. As an example, several 1,12-diazaperylene (DAP)-based Ru^{II} complexes exhibit MLCT absorption maxima in the range of 550–590 nm, but at the sacrifice of $^1O_2$ quantum yield.[5]

[a] Dr. Q.-X. Zhou, W.-H. Lei, J.-R. Chen, C. Li, Y.-J. Hou, Prof. X.-S. Wang, B.-W. Zhang
Key Laboratory of Photochemical Conversion and Optoelectronic Materials
Technical Institute of Physics and Chemistry
Chinese Academy of Sciences
Beijing 100190 (P.R. China)
Fax: (+86) 106-487-9375
E-mail: xswang@mail.ipc.ac.cn
g203@mail.ipc.ac.cn

[b] Dr. Q.-X. Zhou
Graduate School of Chinese Academy of Sciences
Beijing 100049 (P.R. China)

Supporting information for this article is available on the WWW under http://dx.doi.org/10.1002/chem.200902563.

To develop long-wavelength-absorbing Ru polypyridyl complexes, we recently focused our attention on the ligand 2,3-bis(2-pyridyl)benzoquinoxaline (dpb). The highly delocalized π system of the dpb ligand gives the corresponding Ru complex a much longer wavelength MLCT absorption.[8] For example, $[Ru(bpy)_2(dpb)]^{2+}$ (bpy = 2,2′-bipyridine) shows a very long wavelength ^{1}MLCT absorption with a maximum at 550 nm, but a much shortened ^{3}MLCT lifetime (66 ns, result of this work) with respect to $[Ru(bpy)_3]^{2+}$ (450 nm and 900 ns[9]). Thus, it is of importance to lengthen the MLCT lifetime while maintaining the long-wavelength MLCT absorption.

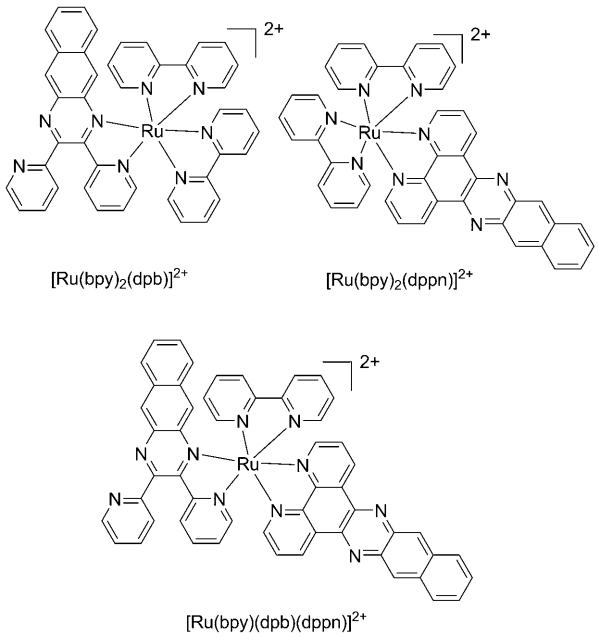

The so-called "reservoir effect" has become a potent measure to lengthen the ^{3}MLCT lifetimes of Ru^{II} complexes.[10] The underlying mechanism is the establishment of a fast equilibration between the ^{3}MLCT state of the complex and the triplet excited state of the attached organic chromophore on the ligand or just the ligand itself, which is very long lived and locates close to ^{3}MLCT in energy.

Thus, ^{1}MLCT excitation results in the population of the triplet excited state of the organic chromophore or ligand, which serves as an energy reservoir to allow the ^{3}MLCT to relax in a much longer time domain. Recently, Turro, Thummel, and co-workers demonstrated that the lowest-energy excited state in $[Ru(pydppn)_{2-n}(tpy)_n]^{2+}$ (pydppn = 3-(pyrid-2′-yl)-4,5,9,16-tetraaza-dibenzo[*a*,*c*]naphthacene, *n* = 0, 1; tpy = 2,2′:6′,2″-terpyridine) is a ligand-centered $^3\pi\pi^*$ state localized on the pydppn ligand with lifetimes of ≈20 μs.[4g] The low-energy and long-lifetime characters of pydppn inspired us to construct a new Ru^{II} complex, $[Ru(bpy)(dpb)(dppn)]^{2+}$ (dppn = 4,5,9,16-tetraaza-dibenzo[*a*,*c*]naphthacene), with the hope that dppn may approach MLCT(Ru→dpb) in triplet excited-state energy and thus may serve as an energy reservoir to extend the ^{3}MLCT(Ru→dpb) lifetime.

Herein, we report the fascinating properties of $[Ru(bpy)(dpb)(dppn)]^{2+}$, which keeps the merit of the long-wavelength absorption of the parent complex $[Ru(bpy)_2dpb]^{2+}$ and also exhibits a relatively long excited-state lifetime (229 ns) and high $^1O_2$ quantum yield (0.43), through benefiting from the interplay of $^3\pi\pi^*$(dppn) and ^{3}MLCT(Ru→dpb). The dppn ligand also gives the complex a strong binding affinity towards double-stranded DNA. As a result, $[Ru(bpy)(dpb)(dppn)]^{2+}$ exhibits DNA photocleavage activity and PDT application potential, thus fully displaying the modular and versatile nature of heteroleptic Ru^{II} complexes.

Results and Discussion

Synthesis: The parent complexes $[Ru(bpy)_2(dppn)][PF_6]_2$ and $[Ru(bpy)_2(dpb)][PF_6]_2$ were easily prepared in good yields (60 and 76%, respectively) through the reaction of $[Ru(bpy)_2Cl_2]$ with dppn or dpb ligands. In contrast, the heteroleptic Ru^{II} complex $[Ru(bpy)(dpb)(dppn)](PF_6)_2$ was synthesized in a stepwise manner, by using $[Ru(dmso)_4Cl_2]$ (dmso = dimethyl sulfoxide) as a precursor and chelating the ligands onto the Ru^{II} core in the sequence of bpy, dppn, and dpb. The three complexes were fully characterized by ^{1}H NMR spectroscopy (Figure S1 in the Supporting Information), mass spectrometry (MS, both MALDI-TOF and ESI), and elemental analysis.

Electrochemical and photophysical properties: The oxidation and reduction potentials of the complexes in CH_3CN are shown in Table 1 (see Figure S2 in the Supporting Information for cyclic voltammograms). $[Ru(bpy)_2(dppn)]^{2+}$ and $[Ru(bpy)_2(dpb)]^{2+}$ display a ruthenium(III/II)-based half-wave oxidation potential at +1.35 and +1.40 V versus SCE, respectively. The anodic shift relative to that of $[Ru(bpy)_3]^{2+}$

Table 1. Photophysical and electrochemical properties and binding constants towards CT-DNA of the examined complexes.

Complex	MLCT Abs$_{max}$[a] [nm]	MLCT Em$_{max}$[b] [nm]	$E_{1/2}$(ox)[c] [V] (vs. SCE)	E_p(red)[d] [V] (vs. SCE)	τ_{TA}[e] [ns]	K_b[f] [$\times 10^7$ M^{-1}]
$[Ru(bpy)_3]^{2+}$	449	615	1.29	−1.33	–	–
$[Ru(bpy)_2(dppn)]^{2+}$	442	620[g]	1.35	−0.85	13000	4.0
$[Ru(bpy)_2(dpb)]^{2+}$	551	927[h]	1.40	−0.67	66	0.17
$[Ru(bpy)(dpb)(dppn)]^{2+}$	548	926[h]	1.52[i]	−0.83, −0.58	229	1.9

[a] MLCT absoption maximum in acetonitrile. [b] MLCT emission maximum in acetonitrile at 298 K. [c] Oxidation half-wave potentials in acetonitrile. [d] Reduction peak potentials in acetonitrile. [e] Excited-state lifetime obtained by transient absorption in CH_3CN. [f] Binding constant obtained by ethidium bromide displacement assay. [g] Measured on a Hitachi F-4500 fluorescence spectrophotometer. [h] Recorded on a NIR fiber-optic spectrometer. [i] Peak potential.

(+1.29 V) is attributable to the more electronegative character or stronger π-accepting feature of dppn or dpb than bpy, reflected in the less negative reduction potentials of −0.85 V for dppn and −0.67 V for dpb compared with −1.33 V for bpy (Table 1). For $[Ru(bpy)(dpb)(dppn)]^{2+}$, the metal-centered oxidation peak potential was measured to be 1.52 V, and the reduction potentials for dppn and dpb are both anodically shifted relative to those in $[Ru(bpy)_2(dppn)]^{2+}$ and $[Ru(bpy)_2(dpb)]^{2+}$, obviously due to the simultaneous presence of the two strong π-accepting ligands. The stronger electron-accepting property of dpb suggests that the lowest-energy ^{3}MLCT in $[Ru(bpy)(dpb)(dppn)]^{2+}$ should localize on the dpb ligand.

Figure 1a shows the normalized absorption spectra of $[Ru(bpy)_2(dppn)]^{2+}$, $[Ru(bpy)_3]^{2+}$, and the dppn ligand. Comparisons among them lead to clear assignments of the absorption transitions of $[Ru(bpy)_2(dppn)]^{2+}$: a bpy ligand-based transition at 286 nm; dppn ligand-based transitions at 323, 387, and 409 nm; and MLCT transitions centered at 442 nm. Interestingly, although dppn coordinated to Ru^{II} is more easily reduced than bpy (see Table 1) and possesses an extended aromatic conjugation system for charge delocalization, the MLCT absorption maximum of $[Ru(bpy)_2(dppn)]^{2+}$ is very similar to that of $[Ru(bpy)_3]^{2+}$. Similar phenomena were also found in comparisons of $[Ru(phen)_2(dppz)]^{2+}$[11] (phen = 1,10-phenanthroline, dppz = dipyrido[3,2-*a*:2′,3′-*c*]-phenazine) versus $[Ru(phen)_3]^{2+}$ or $[Ru(tpy)(pydppn)]^{2+}$[4g] versus $[Ru(tpy)_2]^{2+}$.

$[Ru(bpy)_2(dppn)]^{2+}$ shows an emission spectrum centered at 620 nm in acetonitrile at room temperature (Figure S3 in the Supporting Information), also very similar to that of $[Ru(bpy)_3]^{2+}$, which has an emission peaking at 615 nm under the same conditions. However, the emission intensities of $[Ru(bpy)_2(dppn)]^{2+}$ and $[Ru(bpy)_3]^{2+}$ are very different. The emission quantum yield of $[Ru(bpy)_3]^{2+}$ is 0.062,[9] whereas $[Ru(bpy)_2(dppn)]^{2+}$ emits approximately 60-fold less efficiently than $[Ru(bpy)_3]^{2+}$, with an emission quantum yield of 1.07×10^{-3}. $[Ru(bpy)_2(dppn)]^{2+}$ exhibits a new emission at 821 nm (corresponding to 1.5 eV) along with the ^{3}MLCT emission at 580 nm (corresponding to 2.1 eV) at 77 K in ethanol/methanol (4:1) glass (Figure S4 in the Supporting Information). This new emission is very weak in intensity but highly reproducible. In contrast, no such emission was observed in the case of $[Ru(bpy)_3]^{2+}$ at 77 K. Thus, the new emission presumably comes from the phosphorescence of the dppn ligand (dppn itself does not emit at this wavelength at 77 K, probably due to its low intersystem crossing efficiency and low phosphorescence quantum yield), in accordance with the pydppn ligand, an analogue of dppn, the triplet excited-state energy of which was estimated to be 1.5 eV.[4g] Thus, the remarkably diminished emission quantum yield of $[Ru(bpy)_2(dppn)]^{2+}$ may result from the low energy of the dppn triplet excited state, which lies 0.6 eV below the ^{3}MLCT state and thus quenches ^{3}MLCT emission effectively.

Figure 1b gives the normalized absorption spectra of $[Ru(bpy)_2(dpb)]^{2+}$, $[Ru(bpy)_3]^{2+}$, and the dpb ligand. Comparisons among them give the following assignments for the absorption transitions of $[Ru(bpy)_2(dpb)]^{2+}$: bpy- and dpb-based transitions at 286 and 315 nm; a dpb-based transition

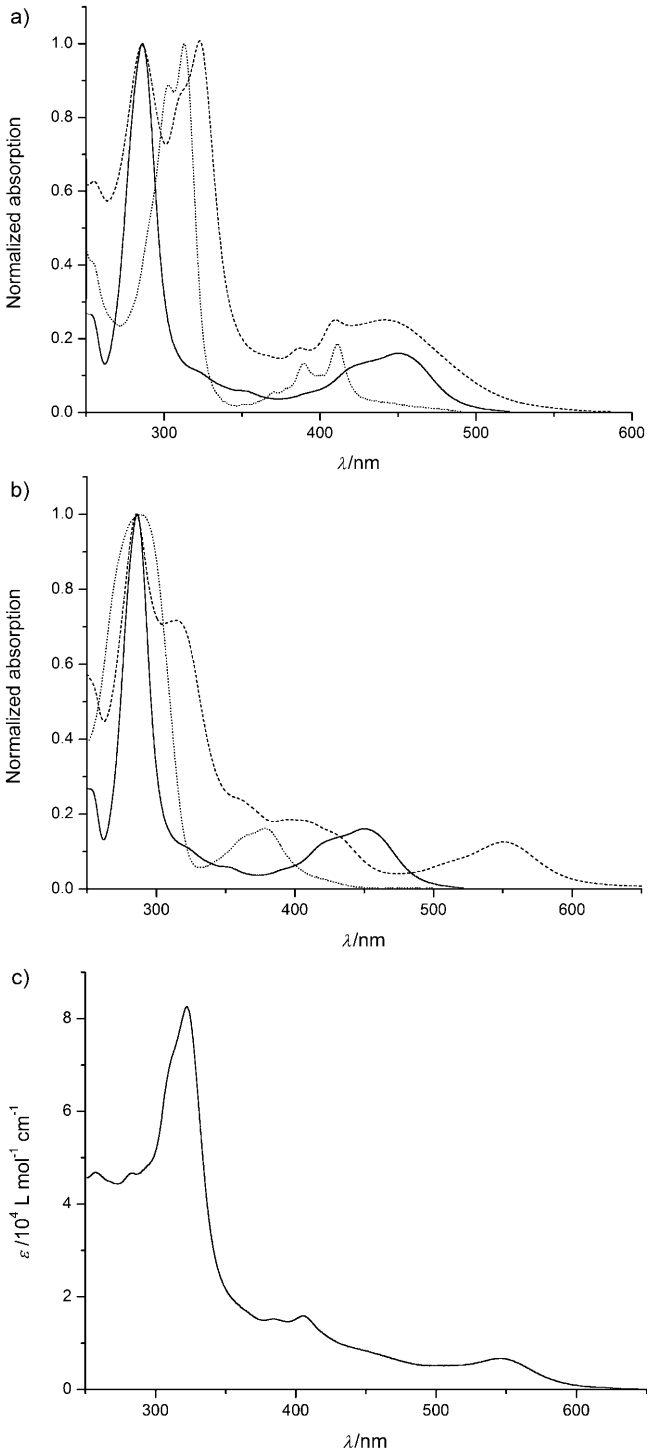

Figure 1. a) Normalized absorption spectra of $[Ru(bpy)_2(dppn)]^{2+}$ (-----), $[Ru(bpy)_3]^{2+}$ (——), and dppn (•••••) in acetonitrile. b) Normalized absorption spectra of $[Ru(bpy)_2(dpb)]^{2+}$ (-----), $[Ru(bpy)_3]^{2+}$ (——), and dpb (•••••) in acetonitrile. c) Absorption spectrum of $[Ru(bpy)(dppn)(dpb)]^{2+}$ in acetonitrile.

at 365 nm; and MLCT transitions centered at 551 nm for Ru→dpb. Greatly different from the dppn ligand, the presence of the dpb ligand makes the corresponding complex $[Ru(bpy)_2(dpb)]^{2+}$ undergo a 100 nm redshift in the MLCT absorption maximum with respect to $[Ru(bpy)_3]^{2+}$, which may be the result of the remarkable anodic shift of the reduction potential of dpb relative to that of dppn (Table 1).

The emission of $[Ru(bpy)_2(dpb)]^{2+}$ extends into the NIR region so that common fluorescence spectrophotometers, such as the Hitachi F-4500 with an emission detection range of 220–730 nm, cannot be used. In our experiments, a NIR fiber-optic spectrometer with the wavelength range of 880–1684 nm was applied to examine the emission of $[Ru(bpy)_2(dpb)]^{2+}$. The excitation light source was a Millennia laser (532 nm output, continuous wave (CW)). An emission with maximum at 927 nm was observed (Figure S3 in the Supporting Information). $[Ru(bpy)_2(dppn)]^{2+}$, $[Ru(bpy)_3]^{2+}$, bpy, dppn, and dpb have no signals under similar conditions, excluding the artifact origin of the observed emission signal. Considering the blueshift of the MLCT emission upon freezing at 77 K by about 40 nm (e.g., $[Ru(bpy)_2(dppn)]^{2+}$ in this work and other Ru^{II} complexes[4e,g]), a 0–0 transition energy of 1.4 eV (corresponding to 887 nm) for the Ru→dpb MLCT transition is estimated. As for the dpb ligand, its triplet excited-state energy is most likely higher than that of dppn, due to its structural similarity to dppn but blue-shifted absorption relative to dppn (Figure 1a and b). The transient absorption spectrum of $[Ru(bpy)_2(dpb)]^{2+}$ also reveals that the lowest-energy state is Ru→dpb ^{3}MLCT rather than the dpb triplet state (see below).

Once the absorption and emission characteristics of $[Ru(bpy)_2(dppn)]^{2+}$ and $[Ru(bpy)_2(dpb)]^{2+}$ are understood, the assignment of the absorption and emission spectra (Figure 1c and Figure S1 in the Supporting Information) of $[Ru(bpy)(dppn)(dpb)]^{2+}$ becomes straightforward. The absorption within the range 250–350 nm originates mainly from the ligand (including all three ligands)-based $^1\pi\pi^*$ transition, that at 350–425 nm is mainly from the dppn/dpb-based $^1\pi\pi^*$ transition, and that above 425 nm is mainly from ^{1}MLCT, with the lowest-energy ^{1}MLCT localized on the dpb ligand (centered at 548 nm). The NIR emission of $[Ru(bpy)(dppn)(dpb)]^{2+}$ is similar to that of $[Ru(bpy)_2(dpb)]^{2+}$. Figure 2 shows simplified Jablonski diagrams for the three complexes on the basis of the energies of the MLCT and ligand-centered excited states.

Time-resolved absorption spectra: Figure 3 shows the transient absorption spectra of $[Ru(bpy)_2(dppn)]^{2+}$ and the dppn ligand in CH_3CN. The high degree of similarity between them suggests that the observed transient spectra of $[Ru(bpy)_2(dppn)]^{2+}$ result from dppn-based triplet–triplet (T–T) absorption, which is in good agreement with the fact that the lowest triplet excited state in $[Ru(bpy)_2(dppn)]^{2+}$ is localized on $^3\pi\pi^*$(dppn) rather than ^{3}MLCT (see the above discussion and Figure 2). The measured lifetimes for $[Ru(bpy)_2(dppn)]^{2+}$ and dppn are 13 and 18 μs, respectively, which are comparable to the lifetimes of $[Ru(tpy)(pydppn)]^{2+}$ (20 μs), $[Ru(pydppn)_2]^{2+}$ (24 μs), and pydppn (22 μs) in degassed acetonitrile.[4g] We also found that tetra-

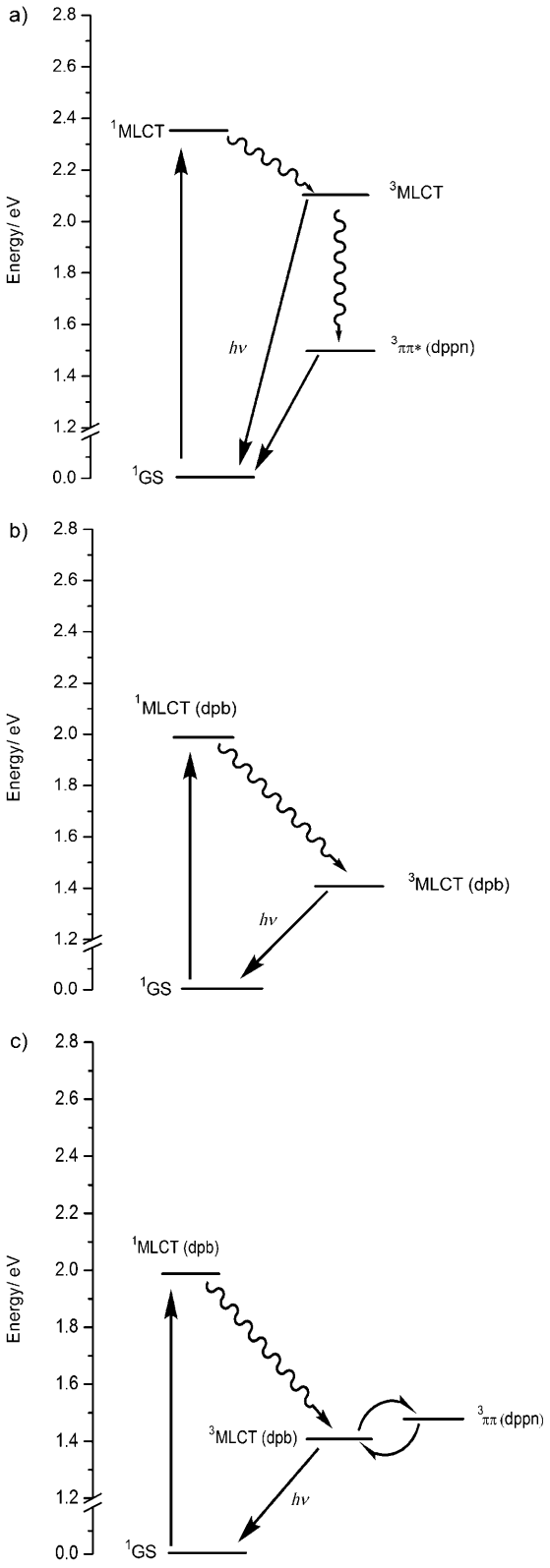

Figure 2. Simplified Jablonski diagrams for a) $[Ru(bpy)_2(dppn)]^{2+}$, b) $[Ru(bpy)_2(dpb)]^{2+}$, and c) $[Ru(bpy)(dppn)(dpb)]^{2+}$.

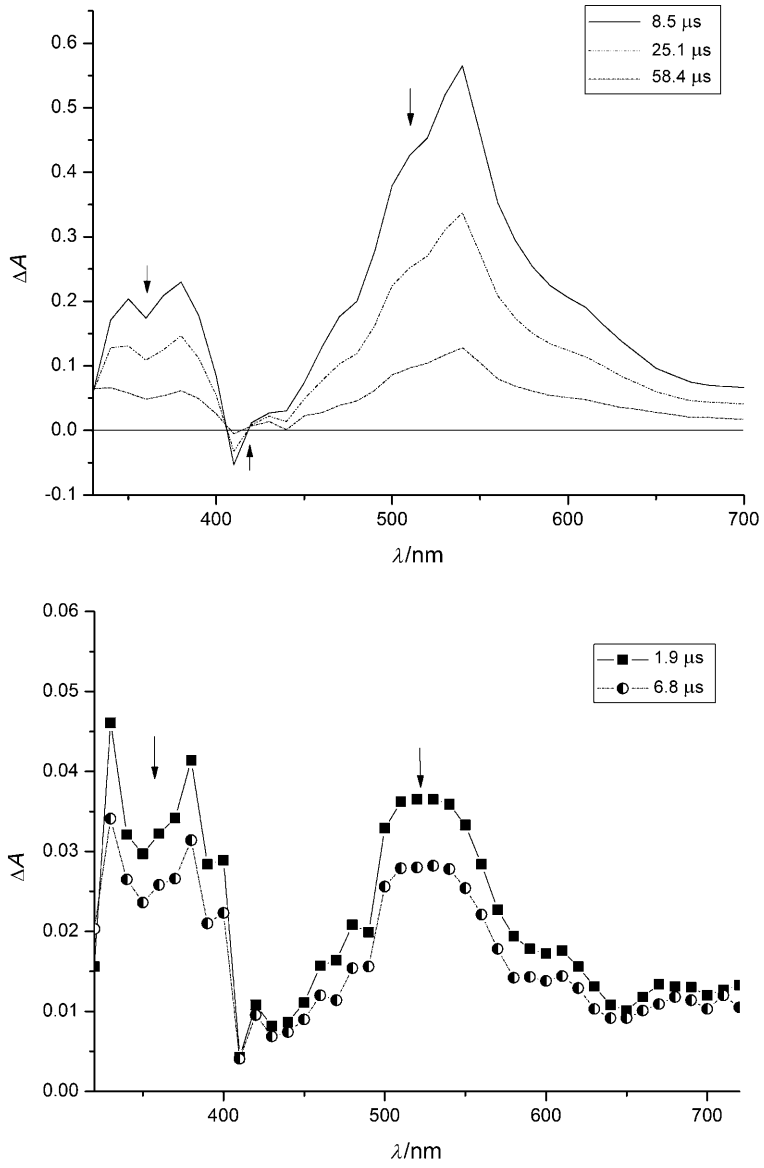

Figure 3. Transient absorption spectra of $[Ru(bpy)_2(dppn)]^{2+}$ (top) and the dppn ligand (bottom) in degassed CH_3CN solution upon illumination at 355 nm with a pulsed laser.

cene (triplet excited-state energy $E_T = 1.27$ eV[4g]) and perylene ($E_T = 1.53$ eV[4g]) can quench the transient absorption spectra of $[Ru(bpy)_2(dppn)]^{2+}$ effectively, with the quenching constants of 7.7×10^9 (tetracene) and $5.4\times10^9\,M^{-1}s^{-1}$ (perylene). In contrast, no quenching was observed in the case of 9,10-dibromoanthracene, the E_T of which is as high as 1.74 eV.[4g] These findings are in good agreement with the estimation of dppn triplet-state energy (1.5 eV).

Figure 4 shows the transient absorption spectra of $[Ru(bpy)_2(dpb)]^{2+}$ and $[Ru(bpy)(dpb)(dppn)]^{2+}$ at 298 K in degassed CH_3CN upon pulsed excitation at 532 nm. $[Ru(bpy)_2(dpb)]^{2+}$ shows a ground-state bleaching band centered at 550 nm, and positive absorption below 515 and over 580 nm, which resembles the typical ^{3}MLCT T–T absorption spectra of Ru^{II} polypyridyl complexes that do not emit or have a low quantum yield of emission,[4e,12] in line with the assignment of the lowest triplet excited state to Ru→dpb ^{3}MLCT in $[Ru(bpy)_2(dpb)]^{2+}$. Single-exponential fitting of the spectrum changes at 650 nm as well as other wavelengths gives a ^{3}MLCT lifetime of 66 ns.

The transient absorption spectrum of $[Ru(bpy)(dpb)(dppn)]^{2+}$ differs significantly from that of $[Ru(bpy)_2(dpb)]^{2+}$. Positive absorption appeared in the whole spectrum window, and no bleaching band was observed. The transient absorption spectrum of $[Ru(bpy)(dpb)(dppn)]^{2+}$ may be regarded as the superposition of those from $[Ru(bpy)_2(dppn)]^{2+}$ and $[Ru(bpy)_2(dpb)]^{2+}$, that is, the bleaching at 550 nm and positive absorption over 600 nm of $[Ru(bpy)_2(dpb)]^{2+}$ makes the transient absorption of $[Ru(bpy)_2(dppn)]^{2+}$ become less undulating in intensity over the wide range of 500–700 nm, thus implying the co-existence of both ^{3}MLCT(Ru→dpb) and $^3\pi\pi^*$(dppn). The close proximity of ^{3}MLCT(Ru→dpb) and $^3\pi\pi^*$(dppn) in energy (1.4 and 1.5 eV, respectively, which corresponds to an energy gap of 806 cm^{-1}) makes this assumption possible.[10] Moreover, a single lifetime of 229 ns was obtained by fitting the decay at different wavelengths, which indicates that both ^{3}MLCT(Ru→dpb) and $^3\pi\pi^*$(dppn) deactivate at the same rate, and suggests the establishment of a fast equilibrium between the two states.[10] From the equilibrated lifetime $\tau_{eq} = 229$ ns, the fraction with populated $^3\pi\pi^*$(dppn) states ($\alpha = 70\,\%$) and the fraction with populated ^{3}MLCT(Ru→dpb) states ($1-\alpha = 30\,\%$) can be estimated on the basis of $\tau_{eq}^{-1} = \alpha\tau_p^{-1} + (1-\alpha)\tau_{Ru}^{-1}$, in which τ_p (= 13 μs) is the lifetime of $^3\pi\pi^*$(dppn) in $[Ru(bpy)_2(dppn)]^{2+}$ and τ_{Ru} (= 66 ns) is the lifetime of ^{3}MLCT(Ru→dpb) in $[Ru(bpy)_2(dpb)]^{2+}$.[10d] Thus, an equilibrium constant $K = 2.33$ and a free energy change $\Delta G = -0.5$ kcal mol^{-1} (corresponding to −0.02 eV) for thermal population from ^{3}MLCT(Ru→dpb) to $^3\pi\pi^*$(dppn) can be calculated. Taking into consideration the possible errors in estimating excited-state energies from both emission spectra and equilibrated lifetime, the ^{3}MLCT(Ru→dpb) and

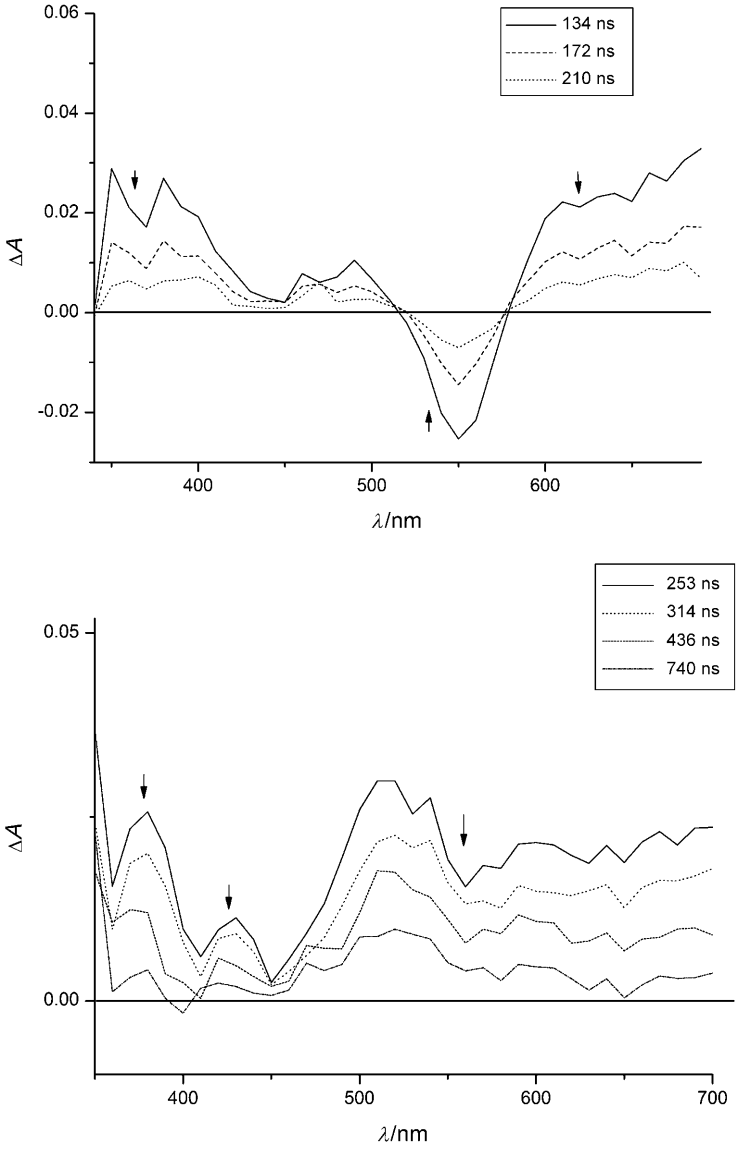

Figure 4. Transient absorption spectra of $[Ru(bpy)_2(dpb)]^{2+}$ (top) and $[Ru(bpy)(dpb)(dppn)]^{2+}$ (bottom) in degassed CH_3CN solution upon illumination at 532 nm with a pulsed laser.

$^3\pi\pi^*$(dppn) states are most likely isoenergetic in $[Ru(bpy)(dpb)(dppn)]^{2+}$.

Additionally, we measured the transient absorption spectra of samples of $[Ru(bpy)(dpb)(dppn)]^{2+}$ containing 5% of $[Ru(bpy)_2(dppn)]^{2+}$ or dppn ($\lambda_{ex}=532$ nm in the case of $[Ru(bpy)_2(dppn)]^{2+}$ or 355 nm in the case of dppn). In such cases, a very long lifetime belonging to $Ru(bpy)_2(dppn)]^{2+}$ (12 μs) or dppn (17 μs) can be detected along with a lifetime of about 220 ns belonging to $[Ru(bpy)(dpb)(dppn)]^{2+}$. The lack of interactions between $[Ru(bpy)(dpb)(dppn)]^{2+}$ and $[Ru(bpy)_2(dppn)]^{2+}$ or between $[Ru(bpy)(dpb)(dppn)]^{2+}$ and dppn may result from the low sample concentration employed (3×10^{-5} M). This result indicates that $[Ru(bpy)(dpb)(dppn)]^{2+}$ is pure enough and no impurity that possesses a long excited-state lifetime, such as the dppn ligand or $[Ru(bpy)_2(dppn)]^{2+}$, exists to interfere with the transient absorption assignment of $[Ru(bpy)(dpb)(dppn)]^{2+}$. Moreover, we compared the $^1O_2$ quantum yields of $[Ru(bpy)(dpb)(dppn)]^{2+}$ at different excitation wavelengths, and no wavelength dependence was observed, thus ruling out further the presence of an impurity with a different $^1O_2$ quantum yield, such as $[Ru(bpy)_2(dppn)]^{2+}$ or dppn. Elemental analysis gave a purity in excess of 99.5% for $[Ru(bpy)(dpb)(dppn)]^{2+}$ based on measured carbon or nitrogen. All these control experiments confirm that the long lifetime of 229 ns originates from $[Ru(bpy)(dpb)(dppn)]^{2+}$, which benefits from the "energy reservoir effect". Previous work on this effect normally involved an appended organic fragment. Here, the organic fragment is part of the coordinating skeleton itself.

$^1O_2$ quantum yield: Singlet oxygen plays an important role in PDT, thus the $^1O_2$ quantum yields of $[Ru(bpy)_2(dppn)]^{2+}$, $[Ru(bpy)_2(dpb)]^{2+}$, and $[Ru(bpy)(dpb)(dppn)]^{2+}$ were determined with $[Ru(bpy)_3]^{2+}$ as the standard ($\Phi=0.57$ in CH_3CN)[13] and 1,3-diphenylisobenzofuran (DPBF) as the trapping agent of $^1O_2$. The $^1O_2$ quantum yields were measured to be 0.79 for $[Ru(bpy)_2(dppn)]^{2+}$, 0.22 for $[Ru(bpy)_2(dpb)]^{2+}$, and 0.43 for $[Ru(bpy)(dpb)(dppn)]^{2+}$ in CH_3CN ($\lambda_{ex}=480$ nm). The $^1O_2$ quantum yield of $[Ru(bpy)(dpb)(dppn)]^{2+}$ is almost two times larger than that of $[Ru(bpy)_2(dpb)]^{2+}$, presumably due to its much longer excited-state lifetime (229 vs. 66 ns). The EPR spin-trapping technique was also used to examine their $^1O_2$ generation abilities. Figure 5 presents the EPR spectra obtained upon irradiation (Nd/YAG laser, 532 nm) of complex samples containing 50 mM 2,2,6,6-tetramethyl-4-piperidone (TEMP), in which TEMP acted as a spin-trapping agent for $^1O_2$. The spectrum is composed of three lines of equal intensity with a hyperfine splitting constant of 16.0 G, identical to the typical EPR signal of 2,2,6,6-tetramethyl-4-piperidone oxide (TEMPO,

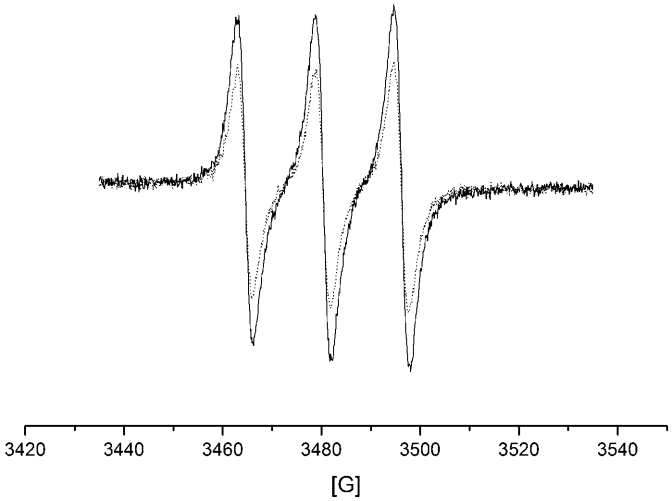

Figure 5. EPR signals obtained upon irradiation with a 532 nm laser of air-saturated CH_3CN solutions containing 50 mM TEMP and 10 μM $[Ru(bpy)(dpb)(dppn)]^{2+}$ (——) or $[Ru(bpy)_2(dpb)]^{2+}$ (•••••).

an adduct of TEMP with $^1O_2$).[14] The quenching of the signal by NaN_3, an effective scavenger for $^1O_2$, vindicates the assignment further (see the Supporting Information). $[Ru(bpy)(dpb)(dppn)]^{2+}$ exhibits a much higher signal intensity than $[Ru(bpy)_2(dpb)]^{2+}$ under the same conditions, further confirming its better $^1O_2$ photosensitization ability. In aqueous solution, the $^1O_2$ generation ability of $[Ru(bpy)(dpb)(dppn)]^{2+}$ is also higher than that of $[Ru(bpy)_2(dpb)]^{2+}$ (see the Supporting Information), the same trend as that in CH_3CN.

DNA binding and photocleavage: At first, a DNA titration approach was used to examine the binding abilities of these complexes towards calf thymus DNA (CT-DNA). $[Ru(bpy)_2(dppn)]^{2+}$ (25 μM) shows 37% hypochromism at 320 nm and 17% hypochromism at 442 nm (both wavelengths related to the absorption transitions of the dppn ligand) when the concentration of added CT-DNA reached 172 μM; meanwhile, 10 and 3 nm bathochromic shifts were observed, respectively. The calculated binding constant K_b is $2.2\times10^6\,M^{-1}$, similar to that of other complexes based on the dppn ligand.[15] For $[Ru(bpy)(dpb)(dppn)]^{2+}$, the absorbance of the MLCT band increased at first and then decreased continuously with the addition of DNA. Such a kind of behavior was also observed for other Ru^{II} complexes, probably due to DNA-induced complex aggregation.[4g,5,16] Thus, the DNA titration approach is not suitable for determining the binding constant of $[Ru(bpy)(dpb)(dppn)]^{2+}$. In the case of $[Ru(bpy)_2(dpb)]^{2+}$, almost no absorption change occurred, thus indicating its poor DNA-binding ability.

The ethidium bromide (EB) displacement assay was carried out to determine the binding affinity of the complexes towards CT-DNA, and the resulting apparent binding constants are listed in Table 1. $[Ru(bpy)_2(dpb)]^{2+}$ presents a binding constant one order of magnitude lower than those of $[Ru(bpy)_2(dppn)]^{2+}$ and $[Ru(bpy)(dpb)(dppn)]^{2+}$, which reveals the role of dppn in binding towards DNA. Additionally, the binding constant of $[Ru(bpy)(dpb)(dppn)]^{2+}$ is about half that of $[Ru(bpy)_2(dppn)]^{2+}$, which suggests that the dpb ligand may impair the binding ability probably due to steric hindrance.

The DNA photocleavage abilities of $[Ru(bpy)_2(dppn)]^{2+}$, $[Ru(bpy)_2(dpb)]^{2+}$, and $[Ru(bpy)(dpb)(dppn)]^{2+}$ were examined by the agarose gel electrophoresis pattern of supercoiled pBR322 DNA upon visible-light irradiation (≥ 470 nm; Figure 6). Control experiments (see the Supporting Information) indicate that the DNA photocleavage has a singlet-oxygen mechanism. $[Ru(bpy)_2(dppn)]^{2+}$ exhibits the most efficient DNA cleavage, due to its highest $^1O_2$ quantum yield and DNA binding constant among the three complexes, which makes up its weak absorption at longer wavelengths. Obvious DNA cleavage was observed for $[Ru(bpy)(dpb)(dppn)]^{2+}$ after irradiation for 40 min. In contrast, negligible DNA cleavage was observed for $[Ru(bpy)_2(dpb)]^{2+}$ under the same conditions, mainly due to its poor DNA binding ability and relatively low singlet-oxygen quantum yield. The three complexes show good photochemical stability under the same irradiation conditions (see the Supporting Information).

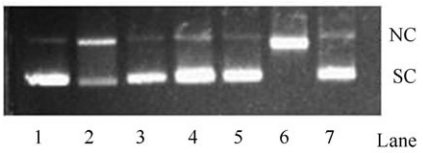

Figure 6. Agarose gel electrophoresis pattern of supercoiled pBR322 DNA (31 μM in base pair) upon visible-light irradiation (≥470 nm) for 40 min (lanes 1, 2, 4, and 6), or dark control (lanes 3, 5, and 7) in air-saturated Tris/CH_3COOH/EDTA buffer (pH 7.4). Lane 1: DNA alone; lanes 2, 3: DNA + $[Ru(bpy)(dpb)(dppn)]^{2+}$; lanes 4, 5: DNA + $[Ru(bpy)_2(dpb)]^{2+}$; lanes 6, 7: DNA + $[Ru(bpy)_2(dppn)]^{2+}$. The concentration of the complex was 8 μM. SC and NC denote supercoiled circular and nicked circular forms, respectively. EDTA: ethylenediaminetetraacetate.

Conclusion

Ru^{II} polypyridyl complexes with long-wavelength absorption and high $^1O_2$ quantum yield are attractive due to their potential use in life and medical sciences, such as PDT. Herein, we reported the synthesis of a heteroleptic Ru^{II} polypyridyl complex, $[Ru(bpy)(dpb)(dppn)]^{2+}$, which keeps the merit of long-wavelength absorption of its parent complex $[Ru(bpy)_2dpb]^{2+}$. The presence of the dppn ligand, on the one hand, lengthens the ^{3}MLCT lifetime from 66 ns for $[Ru(bpy)_2dpb]^{2+}$ to 229 ns, and consequently enhances the $^1O_2$ quantum yield from 0.22 for $[Ru(bpy)_2dpb]^{2+}$ to 0.43; on the other hand, it improves the binding constant towards DNA from $1.7\times10^6\,M^{-1}$ for $[Ru(bpy)_2dpb]^{2+}$ to $1.9\times10^7\,M^{-1}$. As a result, $[Ru(bpy)(dpb)(dppn)]^{2+}$ exhibits DNA photocleavage activity and thus PDT application potential. This work fully demonstrates the advantages of transition-metal complexes, that is, their ease in substitution of the ligands to vary the properties of the complexes and thus to meet individual applications. Ligand modification and the use of different combinations of ligands are in progress to pursue Ru^{II} complexes with longer-wavelength absorption and higher $^1O_2$ quantum yield.

Experimental Section

Materials: Ethidium bromide (EB), 2,2,6,6-tetramethyl-4-piperidone (TEMP), sodium azide (NaN_3), $RuCl_3{\cdot}3H_2O$, 2,3-diaminonaphthalene, 2,2′-bipyridine, 1,10-phenanthroline, 1,3-diphenylisobenzofuran (DPBF), tetra-*n*-butylammonium hexafluorophosphate ($[N(C_4H_9)_4]PF_6$), CT-DNA, gel-loading buffer, tris(hydroxymethyl)aminomethane (Tris base), superoxide dismutase (SOD), and catalase were purchased from Sigma–Aldrich. The supercoiled pBR322 plasmid DNA was purchased from TaKaRa Biotechnology Company.

Synthesis: $[Ru(bpy)_2Cl_2]$,[17] $[Ru(dmso)_4Cl_2]$,[18] dpb,[19] and dppn[20] were synthesized by following the reported methods.

$[Ru(bpy)_2(dppn)][PF_6]_2$: $[Ru(bpy)_2Cl_2]$ (0.30 g) and dppn (0.23 g) were heated at reflux in ethanol/water (2:1, 25 mL) for 3 h under a N_2 atmosphere. The solution was filtered after cooling. After removal of solvent, the solid was purified on silica gel with $CH_3CN/H_2O/KNO_3$ (40:4:1) as

eluent. The compound was dissolved in water and precipitated by NH_4PF_6, and the red solid was isolated by filtration, washed with water, and vacuum dried. Yield 60%; ^{1}H NMR (400 MHz, [D$_6$]acetone): $\delta =$ 7.43–7.45 (m, 2H), 7.63–7.66 (m, 2H), 7.77–7.80 (m, 2H), 8.05–8.09 (m, 2H), 8.15–8.19 (m, 6H), 8.25–8.29 (m, 2H), 8.40–8.43 (m, 2H), 8.51–8.53 (dd, $J=5.3$, 1.2 Hz, 2H), 8.83–8.88 (m, 4H), 9.18 (s, 2H), 9.73–9.76 ppm (dd, $J=8.1$, 1.1 Hz, 2H); MALDI-TOF MS: m/z: 891.26 [$M-PF_6$], 746.42 [$M-2PF_6$]; ESI-MS: m/z: 372.7 $[M-2PF_6]^{2+}$; elemental analysis calcd (%) for $C_{42}H_{28}F_{12}N_8P_2Ru{\cdot}H_2O$: C 47.87, H 2.87, N 10.63; found: C 47.88, H 2.78, N 10.62.

[Ru(bpy)$_2$(dpb)][PF$_6$]$_2$: The synthetic method was similar to that of [Ru(bpy)$_2$(dppn)](PF$_6$)$_2$. Yield 76%; ^{1}H NMR (400 MHz, [D$_6$]acetone): $\delta =$ 7.45–7.48 (m, 2H), 7.56–7.61 (m, 4H), 7.68–7.74 (m, 3H), 7.85–7.93 (m, 2H), 8.06–8.11 (m, 3H), 8.23–8.35 (m, 6H), 8.42–8.48 (m, 3H), 8.56–8.64 (m, 3H), 8.75–8.76 (d, $J=4.3$ Hz, 1H), 8.85 (s, 1H), 8.99–9.03 ppm (m, 2H); MALDI-TOF MS: m/z: 893.17 [$M-PF_6$], 748.18 [$M-2PF_6$]; ESI-MS: m/z: 373.6 $[M-2PF_6]^{2+}$; elemental analysis calcd (%) for $C_{42}H_{30}F_{12}N_8P_2Ru{\cdot}H_2O$: C 47.78, H 3.06, N 10.61; found: C 47.75, H 3.05, N 10.63.

[Ru(bpy)(dpb)(dppn)][PF$_6$]$_2$: The synthesis involved three main steps. First, [Ru(bpy)(dmso)$_2$Cl$_2$] was prepared as follows:[18] [Ru(dmso)$_4$Cl$_2$] (0.5 g) and bpy (0.161 g) were heated at reflux in chloroform (20 mL) for about 45 min under a N_2 atmosphere. After cooling and removal of solvent, the residue was dissolved in acetone and the solution was filtered to remove the residual [Ru(dmso)$_4$Cl$_2$]. The crude product was purified by chromatography on silica gel with CH_2Cl_2/CH_3OH as eluent to obtain the pure compound. Then, pure [Ru(bpy)(dmso)$_2$Cl$_2$] (0.1 g) and dppn (0.069 g) were heated at reflux in ethanol (15 mL) for 4 h under a N_2 atmosphere. After cooling, excess dpb (0.12 g) was added to the solution, which was further heated at reflux for 5 h. After cooling, filtration, and removal of solvent, the solid was purified by chromatography on silica gel with $CH_3CN/H_2O/KNO_3$ as eluent. The compound was dissolved in ethanol/water (1:1) and precipitated by NH_4PF_6, and the dark red solid was isolated by filtration, washed with water, and vacuum dried. Overall yield 10%; ^{1}H NMR (400 MHz, [D$_6$]DMSO): $\delta =$ 7.38–7.45 (m, 1H), 7.47–7.60 (m, 6H), 7.71–7.78 (m, 4H), 7.86–7.88 (d, $J=5.4$ Hz, 1H), 7.95–7.98 (m, 1H), 8.13–8.15 (d, $J=7.4$ Hz, 1H), 8.19–8.41 (m, 10H), 8.48–8.50 (dd, $J=5.4$, 1.04 Hz, 1H), 8.82–8.85 (m, 2H), 8.87–8.88 (dd, $J=4.4$, 1.1 Hz, 1H), 9.04–9.13 (m, 4H), 9.53–9.55 (dd, $J=8.1$, 1.0 Hz, 1H), 9.60–9.63 ppm (dd, $J=8.2$, 1.2 Hz, 1H); MALDI-TOF MS: m/z: 924.5 [$M-2PF_6$]; ESI-MS: m/z: 462.1 $[M-2PF_6]^{2+}$; elemental analysis calcd (%) for $C_{54}H_{34}F_{12}N_{10}P_2Ru{\cdot}H_2O$: C 52.65, H 2.95, N 11.37; found: C 52.62, H 2.91, N, 11.40.

Spectroscopic measurements: ^{1}H NMR spectra were obtained on a Bruker DMX-400 MHz spectrophotometer. ESI and MALDI-TOF mass spectra were determined on a Q-TOF mass spectrometer (Waters) and a Biflex III mass spectrometer (Bruker), respectively. Elemental analysis was performed on an Elementar Vario EL instrument.

UV/Vis absorption spectra were recorded on a Shimadzu UV-1601 spectrophotometer. Emission spectra (300–730 nm) were obtained on a Hitachi F-4500 fluorescence spectrophotometer. NIR luminescence spectra were recorded on a NIR fiber-optic spectrometer (NIR-512-L-1.7T1). The excitation light was from a 532 nm laser obtained from a Tsunami-Spitfire-OPA-800C system (America Optical Spectrum Physics Company, USA) with a Millennia (532 nm, CW) apparatus as laser source.

Redox potentials were measured on an EG&G Model 283 potentiostat/galvanostat in a three-electrode cell with a microdisk Pt working electrode, a Pt-wire counter electrode, and a saturated calomel electrode (SCE) as reference. Cyclic voltammetry was conducted at a scan rate of 150 mV s^{-1} in N_2-saturated, anhydrous CH_3CN containing 0.1 M tetra-*n*-butylammonium hexafluorophosphate as the supporting electrolyte.

EPR spectra were recorded at room temperature on a Bruker ESP-300E spectrometer at 9.8 GHz, X-band with 100 Hz field modulation. Samples were injected quantitatively into quartz capillaries, and illuminated in the cavity of the EPR spectrometer with a Nd/YAG laser at 532 nm (5–6 ns pulse width, 10 Hz repetition frequency, 30 mJ pulse^{-1} energy).

Time-resolved absorption spectra were measured by using the 355 or 532 nm output (5 ns FWHM) from a Nd/YAG laser as pump light, a pulsed flashlamp (Xe 900) as the analyzing light, and a photomultiplier tube (Edinburgh Instruments LP920) for transient detection. Anaerobic conditions were obtained by bubbling the solution with high-purity argon for 20 min. All measurements were carried out at room temperature.

Methods: All experiments involving CT-DNA were performed in phosphate-buffered saline (PBS) solution (pH 7.4). CT-DNA solution was prepared by dispersing the desired amount of DNA in PBS buffer solution with stirring overnight at temperatures below 4 °C. The concentration of CT-DNA was calculated from its absorption at 260 nm with $\varepsilon =$ 6600 M^{-1} cm^{-1}.

The DNA binding constants of the complexes were determined by the absorption titration approach,[21] which was carried out by maintaining a constant metal-complex concentration (25 μM) and increasing the CT-DNA concentration. The binding constants, K_b, were obtained by fitting the titration data to Equations (1) and (2):

$$(\varepsilon_a-\varepsilon_f)/(\varepsilon_b-\varepsilon_f) = [b-(b^2-2K_b{}^2C_t[\mathrm{DNA}]/s)^{1/2}]/2K_bC_t \quad (1)$$

$$b = 1 + K_bC_t + K_b[\mathrm{DNA}]/2s \quad (2)$$

in which ε_f and ε_b are the extinction coefficients at the examined wavelength of the free and bound complex, respectively, ε_a is the apparent extinction coefficient of the complex in the presence of DNA, [DNA] denotes the concentration of DNA in nuclear phosphate, C_t is the concentration of the complex, and s is the binding site size.

The DNA binding constants of the complexes were also determined by EB displacement assay.[22] A solution of EB (2 mL, 5 μM) and CT-DNA (10 μM in base pairs) was titrated with a solution of the complex (0.1 mM in CH_3CN, 5 μL each time), and equilibrated for 10 min before fluorescence measurements (510 nm excitation). The apparent binding affinity was calculated from $K_{EB}[EB] = K_{app}[complex]$, in which [complex] is the concentration of the complex when the EB fluorescence is reduced to 50% of the initial intensity, and K_{EB} is the binding constant of EB towards CT-DNA (1×10^7 M^{-1}).[23]

The DNA photocleavage abilities of the complexes were evaluated by using supercoiled pBR322 plasmid DNA as target. A mixture of supercoiled pBR322 DNA (50 μL, 31 μM in base pair) in PBS buffer (pH 7.4) and the examined complex (5 μL) in CH_3CN (8×10^{-5} M) was irradiated on a "merry-go-round" apparatus for an hour by a medium-pressure sodium lamp (with glass filters $\lambda \geq 470$ nm). After irradiation, gel-loading buffer (15 μL) was added. The sample was then subjected to agarose gel (1%) electrophoresis (Tris/acetic acid/EDTA buffer, pH 8.0) at 80 V for about 2 h. The gel was stained with EB (1 mg L^{-1}) for 45 min, and then analyzed with the Gel Doc XR system (Bio-Rad).

The $^1O_2$ quantum yields of the complexes were determined by using [Ru(bpy)$_3$]$^{2+}$ as the reference ($\Phi = 0.57$ in CH_3CN)[13] and DPBF as the trapping agent of $^1O_2$.[24]

Acknowledgements

This work was financially supported by NNSFC (20772133, 20873170) and CAS (KJCX2.YW.H08).

[1] a) T. J. Dougherty, *Photochem. Photobiol.* **1993**, *58*, 895; b) M. R. Detty, S. L. Gibson, S. J. Wagner, *J. Med. Chem.* **2004**, *47*, 3897; c) T. J. Dougherty, C. J. Gomer, B. W. Henderson, G. Jori, D. Kessel, M. Korbelik, J. Moan, Q. Peng, *J. Natl. Cancer Inst.* **1998**, *90*, 889; d) D. E. J. G. J. Dolmans, D. Fukumura, R. K. Jain, *Nat. Rev. Cancer* **2003**, *3*, 380.
[2] A. Bruce, *Chem. Rev.* **1998**, *98*, 2797.
[3] a) K. E. Erkkila, D. T. Odom, J. K. Barton, *Chem. Rev.* **1999**, *99*, 2777; b) B. M. Zeglis, V. C. Pierre, J. K. Barton, *Chem. Commun.* **2007**, 4565.

[4] a) A. B. Tossi, J. M. Kelly, *Photochem. Photobiol.* **1989**, *49*, 545; b) H. Y. Mei, J. K. Barton, *Proc. Natl. Acad. Sci. USA* **1988**, *85*, 1339; c) H.-B. Arantxa, J.-H. M. Emilia, M. Francisco, O. Esther, O. Guillermo, *J. Phys. Chem. B* **2002**, *106*, 4010; d) H.-Y. Ding, X.-S. Wang, L.-Q. Song, J.-R. Chen, J.-H. Yu, L. Chao, B.-W. Zhang, *J. Photochem. Photobiol. A* **2006**, *177*, 286; e) Y. Liu, R. Hammitt, D. A. Lutterman, R. P. Thummel, C. Turro, *Inorg. Chem.* **2007**, *46*, 6011; f) G. J. Ryan, S. Quinn, T. Gunnlaugsson, *Inorg. Chem.* **2008**, *47*, 401; g) Y. Liu, R. Hammitt, D. A. Lutterman, R. P. Thummel, C. Turro, *Inorg. Chem.* **2009**, *48*, 375; h) Q. X. Zhou, F. Yang, W. H. Lei, J. R. Chen, C. Li, Y. J. Hou, X. C. Ai, J. P. Zhang, X. S. Wang, B. W. Zhang, *J. Phys. Chem. B* **2009**, *113*, 11521.

[5] A. Chouai, S. E. Wicke, C. Turro, J. Bacsa, K. R. Dunbar, D. Wang, R. P. Thummel, *Inorg. Chem.* **2005**, *44*, 5996.

[6] a) P. A. Anderson, F. R. Keene, T. J. Meyer, J. A. Moss, G. F. Strouse, J. A. Treadway, *J. Chem. Soc. Dalton Trans.* **2002**, 3820; b) R. L. Williams, N. Toft, B. Winkel, K. J. Brewer, *Inorg. Chem.* **2003**, *42*, 4394.

[7] R. Englman, J. Jortner, *Mol. Phys.* **1970**, *18*, 145.

[8] a) Y. Y. Ng, C. M. Che, S. M. Peng, *New J. Chem.* **1996**, *20*, 781; b) M. Milkevitch, H. Storrie, E. Brauns, K. J. Brewer, B. W. Shirley, *Inorg. Chem.* **1997**, *36*, 4534; c) M. Milkevitch, B. W. Shirley, K. J. Brewer, *Inorg. Chim. Acta* **1997**, *264*, 249; d) R. L. Williams, H. N. Toft, B. Winkel, K. J. Brewer, *Inorg. Chem.* **2003**, *42*, 4394.

[9] A. Juris, V. Balzani, F. Barigelletti, S. Campagna, P. Belser, A. von Zelewsky, *Coord. Chem. Rev.* **1988**, *84*, 85.

[10] a) X.-Y. Wang, A. D. Guerzo, R. H. Schmehl, *J. Photochem. Photobiol. C* **2004**, *5*, 55; b) R. Passalacqua, F. Loiseau, S. Campagna, Y. Q. Fang, G. S. Hanan, *Angew. Chem.* **2003**, *115*, 1646; *Angew. Chem. Int. Ed.* **2003**, *42*, 1608; c) D. S. Tyson, J. Bialecki, F. N. Castellano, *Chem. Commun.* **2000**, 2355; d) A. F. Morales, G. Accorsi, N. Armaroli, F. Barigelletti, S. J. A. Pope, M. D. Ward, *Inorg. Chem.* **2002**, *41*, 6711; e) D. V. Kozlov, D. S. Tyson, C. Goze, R. Ziessel, F. N. Castellano, *Inorg. Chem.* **2004**, *43*, 6083; f) J. H. Wang, G. S. Hanan, F. Loiseau, S. Campagna, *Chem. Commun.* **2004**, 2068.

[11] C. Hiort, P. Lincoln, B. Norden, *J. Am. Chem. Soc.* **1993**, *115*, 3448.

[12] a) P. S. Braterman, A. Harriman, G. A. Heath, L. Yellowless, *J. Chem. Soc. Dalton Trans.* **1983**, 1801; b) B. Gholamkhass, K. Nozaki, T. Ohno, *J. Phys. Chem. B* **1997**, *101*, 9010; c) B. Gholamkhass, K. Koike, N. Negishi, H. Hori, T. Sano, K. Takeuchi, *Inorg. Chem.* **2003**, *42*, 2919.

[13] A. A. Abdel-Shafi, P. D. Beer, R. J. Mortimer, F. Wilkinson, *J. Phys. Chem. A* **2000**, *104*, 192.

[14] a) Y. Lion, M. Delmelle, A. V. Vorst, *Nature* **1976**, *263*, 442; b) C. Hadjur, A. Jeunet, P. Jardon, *J. Photochem. Photobiol. B* **1994**, *26*, 67.

[15] S. P. Foxon, C. Metcalfe, H. Adams, M. Webb, J. A. Thomas, *Inorg. Chem.* **2007**, *46*, 409.

[16] a) E. Rüba, J. R. Hart, J. K. Barton, *Inorg. Chem.* **2004**, *43*, 4570; b) A. M. Angeles-Boza, P. M. Bradley, P. K.-L. Fu, M. Shatruk, M. G. Hilfiger, K. P. Dunbar, C. Turro, *Inorg. Chem.* **2005**, *44*, 7262; c) Y. Liu, A. Chouai, N. N. Degtyareva, D. A. Lutterman, K. R. Dunbar, C. Turro, *J. Am. Chem. Soc.* **2005**, *127*, 10796.

[17] B. P. Sullivan, D. J. Salmon, T. J. Meyer, *Inorg. Chem.* **1978**, *17*, 3334.

[18] I. P. Evans, A. Spencer, G. Wilkinson, *J. Chem. Soc. Dalton Trans.* **1973**, 204.

[19] H. A. Goodwin, F. Lions, *J. Am. Chem. Soc.* **1959**, *81*, 6415.

[20] V. W.-W. Yam, K. K.-W. Lo, K.-K. Cheung, R. Y.-C. Kong, *J. Chem. Soc. Chem. Commun.* **1995**, 1191.

[21] a) M. T. Carter, M. Rodriguez, A. J. Bard, *J. Am. Chem. Soc.* **1989**, *111*, 8901; b) R. B. Nair, E. S. Teng, S. L. Kirkland, C. J. Murphy, *Inorg. Chem.* **1998**, *37*, 139.

[22] a) Y.-Y. Liu, Q.-X. Zhou, Zh.-H. Zeng, R. Qiao, X.-S. Wang, B.-W. Zhang, *J. Phys. Chem. B* **2008**, *112*, 9959; b) S. E. Wellmann, *Biopolymers* **1996**, *39*, 491.

[23] D. N. A. Boobbyer, P. J. Goodford, P. M. McWhinnie, R. C. Wade, *J. Med. Chem.* **1989**, *32*, 1083.

[24] R. H. Young, K. Wehrly, R. L. Martin, *J. Am. Chem. Soc.* **1971**, *93*, 5774.

Received: September 17, 2009
Revised: December 4, 2009
Published online: January 27, 2010

